BRDF CORRECTION FOR LANDSAT TM/ETM+ DATA OVER AMAZONIAN FORESTS

Jasper Van doninck and Hanna Tuomisto

Department of Biology, University of Turku, Turku, Finland; jasper.vandoninck@utu.fi

ABSTRACT

Radiometric normalization for solar angle and view angle is indispensable when the aim is to identify floristic patterns in tropical forests using high-resolution satellite imagery. However, most routinely generated Landsat products do not correct for the effects of surface reflectance anisotropy. Here we assess these effects over Amazonian forests and compare four different methods of image normalization, using a large number of Landsat images. Two of the methods are Landsat-based and entirely empirical, the other two use the parameters of the semi-empirical MODIS BRDF model. Our results show that all four methods significantly reduce the effect of surface reflectance anisotropy. However, the methods based on MODIS BRDF model parameters result in a systematic undercorrection for the near and shortwave infrared bands.

INTRODUCTION

Although reflectance as measured by spaceborne sensors is mainly determined by surface and atmospheric properties, it is also affected by the angular configuration of the sun, sensor and land surface. This relationship is known as the bidirectional reflectance distribution function (BRDF). It has been studied intensively for sensors with wide swath (1), such as MODIS (with scan zenith angle up to 60°). BRDF-corrected products are routinely generated for these sensors, because then surface reflectances at the edges of a swath can differ strongly from the reflectance at nadir even when the surface is actually uniform. For narrow swath sensors (such as Landsat, with scan zenith angle of 7.5°), the influence of the BRDF is much less pronounced, and a Lambertian surface behaviour is usually assumed in routinely generated surface products (2). This may be adequate when the surface features of interest are spectrally well separable. However, problems arise if the spectral differences among the surface features of interest are subtle, as when the aim is to discriminate among floristically different but structurally similar rainforest types in the Amazon basin. Then any radiometric distortion can introduce errors in image interpretation or classification. The purpose of this study is to find an efficient method for BRDF correction of Landsat images over Amazonian forests.

METHODS

Study area and datasets

The study area consisted of lowland Amazonian rainforest spanning 10 degrees of latitude on both sides of the equator and ranging from 80°W to 50°W (Fig. 1). Within this general area, we used visual interpretation of remotely sensed images to identify regions that were dominated by primary forests. Small settlements and minor roads could be present in the study sites, but we avoided areas at the fringes of the Amazon biome where anthropogenic influences, such as deforestation, have a major effect on the land cover. We also avoided the broad inundated zones adjacent to the Amazon River and its major tributaries, as well as regions with pronounced topographical differences.

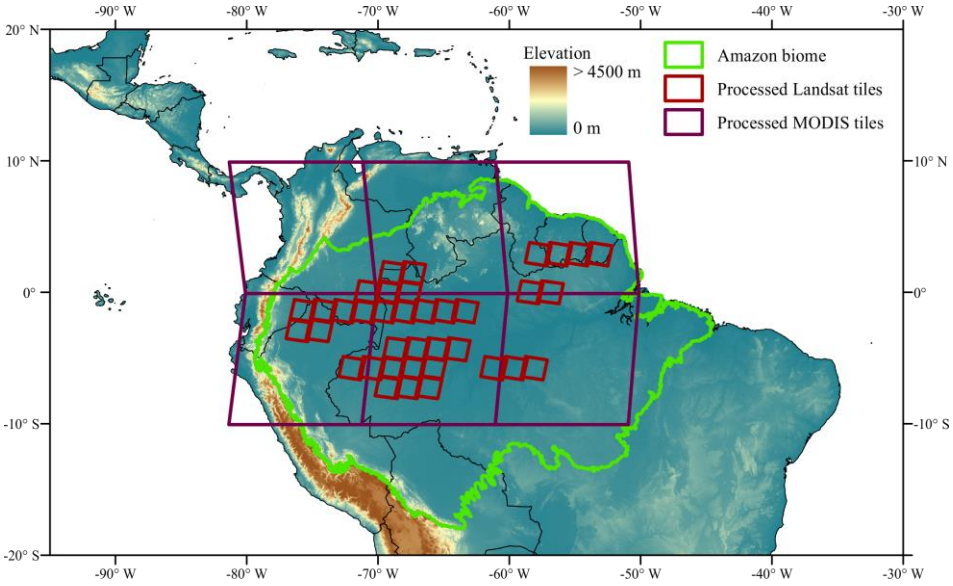

Figure 1: SRTM digital elevation model of the study area.

We used the Landsat Climate Data Record (CDR) surface reflectance high level data products, which are generated using the Landsat Ecosystem Disturbance Adaptive Processing System (LEDAPS) algorithm (2). LEDAPS applies the Second Simulation of a Satellite Signal in the Solar Spectrum (6S) radiative transfer models (3) on Landsat Level-1 products, combined with estimates for ozone concentration, water vapour, elevation and aerosol optical thickness. LEDAPS ignores variation in BRDF and explicitly assumes a Lambertian surface.

We used the USGS EarthExplorer portal (earthexplorer.usgs.gov) to select Landsat TM and ETM+ CDR products (Version 5.5, January 2015) for the 37 WRS-2 scenes that matched our terrain criteria (Fig. 1). Temporally, these acquisitions ranged from the first available Landsat 4 images in 1984 to Landsat 7 images from December 2014. Landsat ETM+ data were used from both before and after the scan line corrector failure. The maximum cloud cover threshold in the EarthExplorer portal was set to 20%. We only downloaded images generated from Level-1 standard terrain correction products (L1T) in order to minimize geometric errors.

Landsat CDR surface reflectance bands are accompanied by several mask bands, which we used to make sure only appropriate pixels were used in the analyses. For each image separately, we excluded all pixels flagged as fill value, cloud cover, adjacent cloud cover, cloud shadow, land water, or any of the mask values in the fmask (4). Additionally, we masked all pixels with an NDVI below 0.5 to remove residual cloud or water cover, roads and settlements. Images left with fewer than 1 million pixels were discarded from further analyses to guarantee that all analyzed images contained a sufficient angular range. In total, the Landsat TM/ETM+ dataset contains 1974 images. Solar zenith (θ) and azimuth were calculated for each pixel using an astronomical model (5) based on the pixel's latitude and longitude and the date and time at the scene centre as supplied in the image metadata. Sensor zenith (ϑ) and azimuth for each pixel were calculated assuming a sensor height of 705 km. The relative azimuth angle (ϕ) was defined as the difference between the solar and sensor azimuth.

MODIS BRDF model parameters for the reflective bands are stored in the MCD43A1 BRDF/Albedo Model Parameters product. Every 8 days, this product provides the weighting parameters for the isotropic, volumetric and geometric kernels (1) calculated using combined Aqua/Terra measurements over a period of 16 days. The corresponding BRDF quality parameters are provided in the combined 8-day product MCD43A2. Both products cover an area of approximately 10° by 10° at a spatial resolution of 500 m, in a sinusoidal projection. MODIS bands 1, 2, 3, 4, 6 and 7 can be considered equivalent to TM/ETM+ bands 3, 4, 1, 2, 5 and 7, respectively. We

downloaded the MCD43A1 and MCD43A2 products (Version 005) for the 6 tiles that cover the Landsat scenes we used (Fig. 1). The data covered twelve years (2002 to 2013).

Landsat-based BRDF correction

BRDF introduces a reflectance gradient in the shortwave wavebands, such that reflectance decreases from the western to the eastern edge of each Landsat scene. This relationship between surface reflectance and position within the Landsat scene has been found to be linear (6) and it can be expressed as:

$$\rho = \alpha\vartheta + \beta$$

where ρ is the surface reflectance for a spectral band in a given pixel. The coefficients α and β can be obtained through linear regression between surface reflectance and sensor zenith angle for the spectral band in question, and α can subsequently be used to normalize each Landsat image to nadir viewing geometry. This normalization method is hereafter referred to as method 'L1'.

We plotted the α values for all images in the dataset against the product of the corresponding cosines of solar zenith angle and relative azimuth angle (Fig. 2). A significant positive relationship exists for all spectral bands, with exception of the blue band. This relationship can be used to estimate the value of α for any combination of solar zenith and relative azimuth angles, and subsequently this estimated α can be used to normalize each Landsat image in respect to viewing geometry. This method is hereafter referred to as 'L2'. The advantage over method L1 is that L2 is less influenced by image-specific perturbing factors, such as spatially heterogeneous land cover or residual atmospheric contamination.

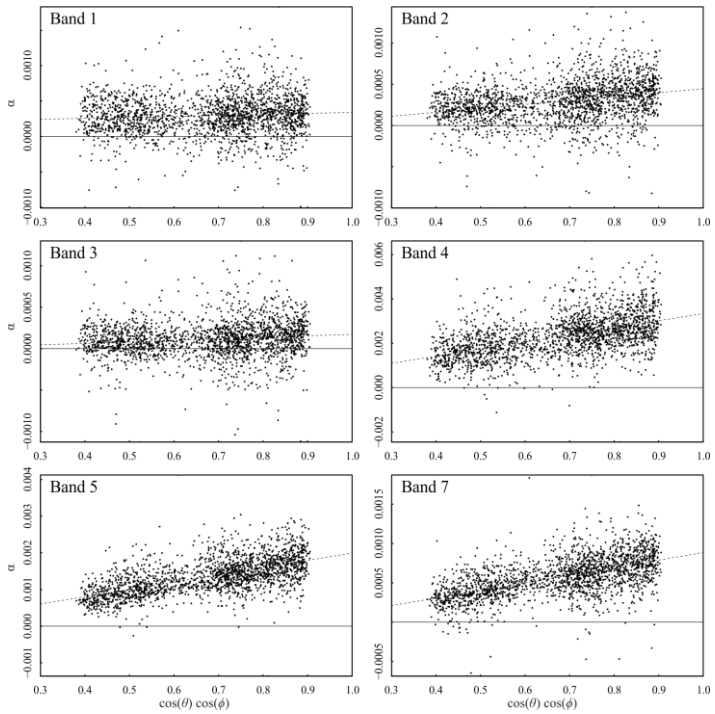

Figure 2: Relationship between the magnitude of the empirical Landsat reflectance gradient (α) and the product of the cosines of solar zenith angle (θ) and relative azimuth angle (ϕ).

MODIS-based BRDF correction

The semiempirical MODIS BRDF model expresses land surface reflectance as the sum of components representing isotropic scattering, volumetric scattering and geometric-optical surface scattering (1). The model parameters are fitted empirically using multitemporal, multiangular observations from the Terra and Aqua platforms during a 16-day period. Given a set of BRDF model parameters, the observed MODIS directional surface reflectance can be transformed to derive normalized reflectance that corresponds to standard solar and satellite angles. Because the

wavelengths of Landsat and MODIS bands are rather similar, the MODIS BRDF parameters can also be used to normalize Landsat imagery. Two different approaches are used here: the first (method 'M1') uses a single set of parameters for the entire Landsat image (7), and the second (method 'M2') uses the parameters of the MODIS pixel that correspond to the Landsat pixel being normalized (8).

A major problem in applying the MODIS-based methods over tropical forests is the persistent cloud cover. MODIS BRDF products can only be generated if a large enough number of cloud-free MODIS acquisitions exist within a 16-day period, and they may not be available for the dates corresponding to an occasional cloud-free Landsat acquisition. We developed a method to circumvent this problem using a time series analysis, which gave us an interpolated set of MODIS parameters for each Landsat acquisition date. The method makes two assumptions. Firstly, the land cover in the study area needs to be stable over the entire time period considered. Therefore, we selected Landsat scenes specifically over primary forests in areas that have not suffered much from deforestation or other human activities. Secondly, it is assumed that any seasonal phenological changes in the vegetation within the study area have a regular temporal pattern and their magnitude is similar over the different years considered. Phenological changes in our study area are in general small, so we find this assumption reasonable.

Accuracy assessment

We assessed BRDF adjustment accuracy using the overlap area of neighbouring Landsat scenes with the same row and adjacent paths. To minimize the effect of surface changes due to phenology, we only compared scenes whose acquisition dates were at most 30 days apart. Both images also had to have enough (minimum 1000) unmasked pixels in the overlap area. In order to reduce the effect of slight differences in georeferencing between the two images in a pair, the spatial resolution was reduced from 30 m to 90 m. The overall performance of each normalization method was assessed by calculating the mean absolute difference (MAD) between reflectance values obtained after normalization and without normalization in the overlap area of each image pair. Systematic over- or undercorrection was assessed by calculating the average surface reflectance in the overlap area of the western image minus that of the eastern image. These values were then averaged over all image pairs covering the same WRS-2 scene combination to obtain a single measure of bias for each image pair. A negative bias is indicative of a systematic undercorrection, a positive bias of overcorrection.

RESULTS

From the original dataset of 1974 Landsat images, we were able to form 1289 pairs fulfilling the requirements (adjacent rows, at most 30 days apart). The mean absolute within-pair reflectance differences for the original values and those obtained with the four normalization methods (MAD) are summarized in Fig. 3. All normalization methods succeeded in reducing the influence of surface reflectance anisotropy, and at least halved the mean absolute difference in reflectance between neighbouring images for the infrared bands. The two Landsat-based methods (L1 and L2) performed significantly better than the two MODIS-based methods (M1 and M2), but the difference between L1 and L2 was not significant, and neither was the difference between M1 and M2 (all based on paired t-test at $p = 0.01$). The effects or BRDF correction are less pronounced for the visible bands, but all four methods still resulted in a significant reduction of MAD in the blue (TM/ETM+ band 1) and green (TM/ETM+ band 2) wavelengths.

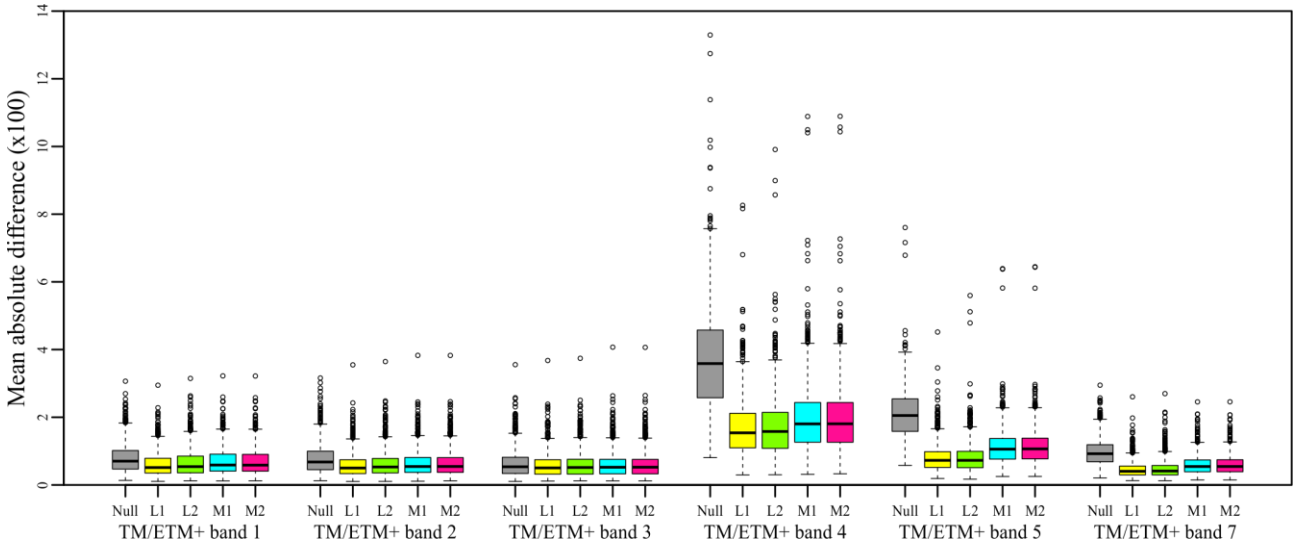

Figure 3: Mean absolute differences between overlap areas in two neighbouring TM/ETM+ images for the original reflectances (null method) and four BRDF normalization methods for each wavelength band.

In Fig. 4, it can be seen that the higher mean absolute differences in the infrared bands (4, 5 and 7) for the MODIS-based BRDF correction are caused by a systematic undercorrection, as indicated by the consistently negative biases. While the bias for methods L1 and L2 approximately equals zero, method M1 and M2 only succeed in approximately halving the bias of the null method.

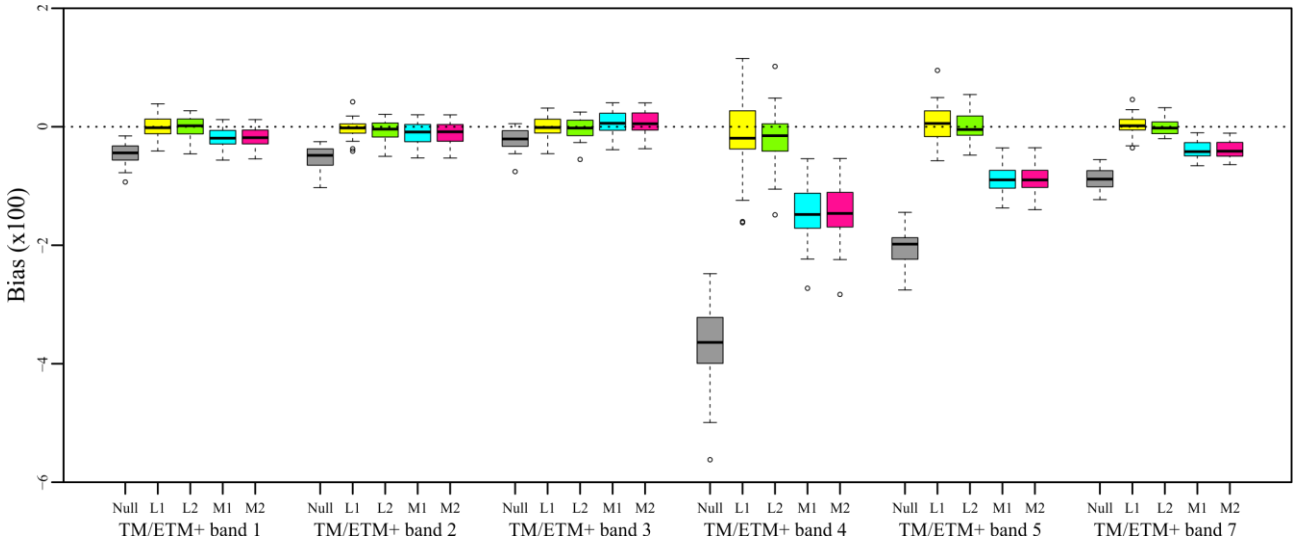

Figure 4: Bias in the difference between overlap areas in two neighbouring TM/ETM+ images for the original reflectances (null method) and four BRDF normalization methods for each wavelength band.

Both Landsat-based approaches (L1 and L2) succeeded in normalizing view angle effects about equally well in terms of mean absolute difference. Overall, bias was small for both methods but slightly closer to zero for L2 than for L1. It should be noted that the MODIS-based methods M1 and M2 normalize surface reflectance to a standard viewing and solar geometry, whereas the empirical Landsat-based corrections can only normalize for view zenith angle. This may become problematic in studies where images acquired in different seasons are compared.

CONCLUSIONS

In this study, we investigated the influence of surface reflectance anisotropy on Landsat imagery over Amazonian forests and evaluated the performance of four normalization methods to reduce that influence. We found that the near infrared band of uncorrected images had a surface reflectance difference of approximately 4% between the western and the eastern edge. In the other reflective bands, the difference was smaller but still significant. All correction methods that we investigated succeeded in reducing the directional effects, although the methods using MODIS BRDF parameters resulted in a systematic undercorrection for the three infrared bands. From a theoretical point of view, the approach has potential, so further research should aim to clarify the causes of this undercorrection and find remedies for it. In addition, the use of MODIS BRDF parameters in normalization of Landsat images should be tested in other parts of the world and over different landcovers. It would also be of interest to investigate how Landsat images normalized to a zenith viewing geometry using the Landsat-based methods could be further normalized to a standard sun-sensor geometry.

ACKNOWLEDGEMENTS

This research was funded by a grant from the Academy of Finland to HT. Image analyses were carried out using the computing facilities provided by CSC-IT Center For Science.

REFERENCES

1 Lucht W, C B Schaaf & A H Strahler, 2000. An algorithm for the retrieval of albedo from space using semiempirical BRDF models. IEEE Transactions on Geoscience and Remote Sensing, 38: 977-998

2 Masek J G M, E F Vermote, N E Saleous, R Wolfe, F G Hall, K F Huemmrich, F Gao, J Kutler & T Lim, 2006. A Landsat surface reflectance dataset for North America, 1990–2000. IEEE Geoscience and Remote Sensing Letters, 3: 68-72

3 Vermote E F, D Tanre, J L Deuze, M Herman & J J Morcrette, 1997. Second Simulation of the Satellite Signal in the Solar Spectrum, 6S: An overview. IEEE Transactions on Geoscience and Remote Sensing, 35: 675-686.

4 Zhu Z, C E Woodcock, 2012. Object-based cloud and cloud shadow detection in Landsat imagery. Remote Sensing of Environment, 118: 83-94

5 Reda I., A Andreas, 2003. Solar Position Algorithm for Solar Radiation Applications. NREL Report No. TP-560-34302, Revised January 2008

6 Hansen M C, D P Roy, E Lindquist, B Adusei, C O Justice & A Altstatt, 2008. A method for integrating MODIS and Landsat data for systematic monitoring of forest cover and change in the Congo Basin. Remote Sensing of Environment, 112: 2495-2513.

7 Li F, D L B Jupp, S Reddy, L Lymburner, N Mueller, P Tan & A Islam, 2010. An Evaluation of the Use of Atmospheric and BRDF Correction to Standardize Landsat Data. IEEE Journal of Selected Topics in Applied Earth Observations and Remote Sensing, 3:257-270

8 Roy D P, J Ju, P Lewis, C Schaaf, F Gao, M Hansen, E Lindquist, 2008. Multi-temporal MODIS-Landsat data fusion for relative radiometric normalization, gap filling, and prediction of Landsat data. Remote Sensing of Environment, 112:3112-3130